Electronic and magnetic properties of (La-Dy)$_{0.7}$Ca$_{0.3}$MnO$_3$

T. Terai, T. Kakeshita, T. Fukuda, and T. Saburi

Department of Materials Science and Engineering, Faculty of Engineering, Osaka University, Suita, Osaka 565-0871, Japan

N. Takamoto and K. Kindo

Research Center for Materials Science at Extreme Conditions, Osaka University, Toyonaka, Osaka 560-8531, Japan

M. Honda

Department of Physics, Faculty of Science, Naruto University of Education, Naruto, Tokushima 772-8502, Japan

Electronic and magnetic properties of the perovskitelike compounds of $(La_{1-x}Dy_x)_{0.7}Ca_{0.3}MnO_3$ ($0 \leq x \leq 0.5$) have been studied by measuring electrical resistivity, magnetic susceptibility, magnetization, and magnetoresistance. All the compounds except $x=0.5$ show a ferromagnetic metal-paramagnetic insulator transition at T_C. T_C of the present compounds depend on the tolerance factor t and when t is larger than 0.913 the relations between T_C and t are almost the same as those observed in the perovskitelike compounds previously examined, which contain rare-earth metal ions, such as Y^{3+}, Pr^{3+}, and Tb^{3+}. When t is smaller than 0.907, a spin glass insulator appears at low temperature. This insulator is different from the ferromagnetic insulator that appears in the compounds containing light rare-earth metal ions, such as Pr^{3+} and/or Y^{3+}, but the same as that appears in the compound containing heavy rare-earth ions of Tb^{3+}. It has been found that, when t takes a value between 0.907 and 0.913, the reentrant spin-glass state appears. Colossal magnetoresistance and tunneling magnetoresistance are clearly observed in the compounds. [S0163-1829(98)00545-1]

I. INTRODUCTION

Perovskite manganites with 20–40 % of trivalent rare-earth ions of R^{3+} replaced by divalent alkaline-earth metal ions of A^{2+}, $R_{1-x}A_xMnO_3$, have been studied for many years and are found to show interesting phenomena, such as metal-insulator transition and colossal magnetoresistance (CMR).[1–10] These phenomena have been mainly explained by double-exchange interaction, magnetic interaction between Mn^{3+} and Mn^{4+} that is caused by the hopping of e_g electrons between the two partially filled d shells with strong on-site Hund's coupling.[11–13]

Recently Hwang *et al.*[3] have investigated $(La_{1-x}R_x)_{0.7}Ca_{0.3}MnO_3$ systematically by replacing some of La^{3+} with Pr^{3+} and/or Y^{3+} and fixing the ratio of Mn^{3+}/Mn^{4+} at 7/3. They found that T_C and conductivity decrease with increasing the content of Pr^{3+} and/or Y^{3+}. Considering these results, they concluded that the electronic and magnetic states of $(La_{1-x}R_x)_{0.7}Ca_{0.3}MnO_3$ depend on the tolerance factor t and established a phase diagram (T_C-t relation). Incidentally the tolerance factor, a geometrical index, is defined as $t=(r_A+r_O)/\sqrt{2}(r_{Mn}+r_O)$, where r_A is the average ionic radius of R^{3+} and Ca^{2+}, r_O is the ionic radius of O^{2-}, and r_{Mn} is the average ionic radius of Mn^{3+} and Mn^{4+}. This factor represents the microscopic distortion from the ideal cubic perovskite structure ($t=1$). With decreasing t, Mn-O-Mn bond angles, which are microscopically related to transfer integral b describing electron hopping between Mn^{3+} and Mn^{4+}, decrease.

The above phase diagram[3] is only derived from the results of the compounds containing light rare-earth metal ions. Thus it is not certain whether or not the above phase diagram holds for the other compounds, especially those containing heavy rare-earth ions. However, few studies have been done on this problem so far.[9,14,15] In the present study, therefore, by replacing La^{3+} with heavy rare-earth ions of Dy^{3+}, we have investigated electronic and magnetic states of $(La_{1-x}R_x)_{0.7}Ca_{0.3}MnO_3$ by measuring electrical resistivity, magnetic susceptibility, magnetization, and magnetoresistance in order to solve the above problem.

II. EXPERIMENT

Polycrystalline specimens of $(La_{1-x}Dy_x)_{0.7}Ca_{0.3}MnO_3$ ($0 \leq x \leq 0.5$) were prepared by conventional solid-state reaction processing in air. In this paper, we describe the compounds using x together with the tolerance factor t for simplicity and in the present case the increase in x corresponds to the decrease in t. Stoichiometric compounds of La_2O_3, Dy_2O_3, $CaCO_3$, and Mn_3O_4 were mixed for the compositions mentioned above and calcined in air by holding the specimens at 1273 K for 12 h. Sintering was carried out in air by holding the specimens at 1623 K for 48 h after intermediate grinding. Powder x-ray-diffraction measurement was made for all the compounds using Rigaku RINT2500. Resistivity ρ was measured by the standard four-probe method for the specimens of 10 mm $\times$ 1.5 mm $\times$ 1 mm. In the measurement, current and voltage leads were connected to the specimen with silver paste. Magnetization was measured by applying static magnetic fields up to 1.8 T and also by applying pulsed high magnetic fields up to 53 T. Magnetoresistance was measured by using the same specimens as those used for the electrical resistivity measurement in zero field. In the magnetoresistance measurement, magnetic fields generated
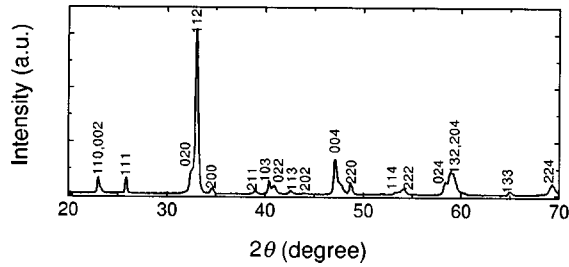
FIG. 1. X-ray-diffraction pattern at room temperature for $(La_{1-x}Dy_x)_{0.7}Ca_{0.3}MnO_3$ $(x=0.5)$.

by superconducting magnet were applied up to 8 T parallel to the constant current.

III. RESULTS

We made powder x-ray-diffraction measurements for all the compounds at room temperature. We found that all the specimens are a single phase of the expected compound and the structure changes from pseudocubic to orthorhombic ($b > c/\sqrt{2} \geqslant a$, O-type) structures as Dy content, i.e., x, increases. A typical diffraction pattern for $x=0.5$ $(t=0.916)$ is shown in Fig. 1, where all the reflections can be indexed by the orthorhombic O-type structure.

Then, we measured the electrical resistivity ρ as a function of temperature (heating and cooling) for all the compounds and the results are shown in Fig. 2. The figure shows that all the compounds except $x=0.5$ $(t=0.916)$ do a metal-insulator transition. The transition temperature T_{IM} is obtained as the temperature where $d \log \rho/dT$ is maximum (indicated with an arrow on each heating curve), which is phenomenologically derived and shown to be almost identical with Curie temperature T_C by Hwang et $al.$[3] A characteristic feature is that T_{IM} decreases with increasing x (decreasing the tolerance factor t mentioned above) and goes to below 1.5 K for $x=0.5$ $(t=0.898)$. This is the same as the behavior of those compounds that contain light rare-earth metal ions, such as Pr^{3+} and/or Y^{3+}.[3] Another characteristic feature is that the resistivities of $x=0.143$, 0.243, and 0.286 $(t=0.911, 0.908,$ and 0.907) increase again at tem-
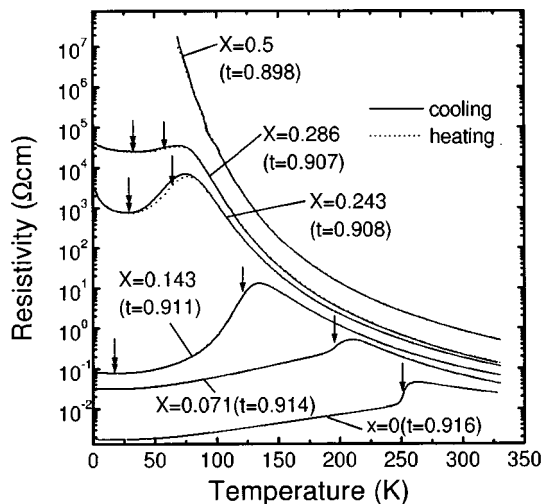

FIG. 2. Temperature dependence of resistivity for $(La_{1-x}Dy_x)_{0.7}Ca_{0.3}MnO_3$ $(0 \leqslant x \leqslant 0.5)$.
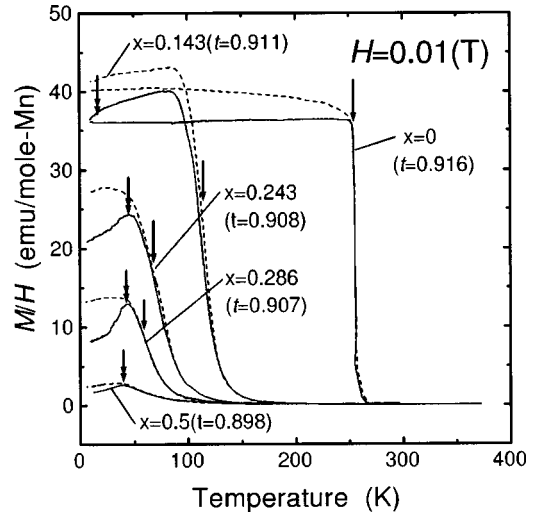
FIG. 3. Temperature dependence of M/H for $(La_{1-x}Dy_x)_{0.7}Ca_{0.3}MnO_3$ $(0 \leqslant x \leqslant 0.5)$ obtained by ZFC (solid line) and FC (dotted line) runs at 0.01 T.

peratures indicated with double arrows. Such increase has not been observed in the compounds containing light rare-earth metal ions only.[3]

In order to obtain more information on this behavior and magnetic states of the compounds, we made measurements on the magnetization (M) for all the compounds under the two conditions; one is the zero-field-cooled (ZFC) run and the other is field-cooled (FC) run at $H=0.01$ T. Then, we plotted M/H against temperature, which is shown in Fig. 3, where solid and dotted curves represent the results of ZFC and FC runs, respectively. T_C is determined as a temperature where $d(M/H)/dT$ is minimum (indicated with an arrow on each curve). This temperature corresponds to Curie temperature obtained by conventional Arrott plot and also corresponds to T_{IM}. It should be noted in the figure that the temperature dependence of M/H obtained by a ZFC run is quite different from that obtained by a FC run at temperatures lower than T_C for all the compounds. Such difference in the compound of $x=0$ $(t=0.916)$ is due to the magnetic domain rotation that will be described later. On the other hand, the difference for the other compounds is believed to be due to a spin glass state which appears for low temperatures. Similar temperature dependences of M/H due to the spin glass state have been observed also for other compounds, such as $(La-Tb)_{2/3}Ca_{1/3}MnO_3$ and Fe-Au (Refs. 9 and 16) (neutron diffraction and ac susceptibility were done to confirm the spin-glass state). According to the previous studies,[9,16] the glass transition temperature T_g is determined as a temperature where M/H-T curve of the ZFC run yields a cusp in cases that T_C and T_g are close each other or identical. This situation holds for the present compounds of $x = 0.243$, 0.286, and 0.5 $(t=0.908, 0.907,$ and 0.898) and, therefore, T_g is obtained as the temperature of the observed cusp, which is shown in each M/H-T curve with the double arrow. On the other hand, for the compound of $x = 0.143$ $(t=0.911)$, the M/H-T curve under a ZFC run has two cusps [one is located at about 90 K, the other is located about 20 K (indicated with the double arrow)], being quite similar to that of a compound that becomes a typical reentrant spin glass at low temperature.[16] In this case, T_g is de-
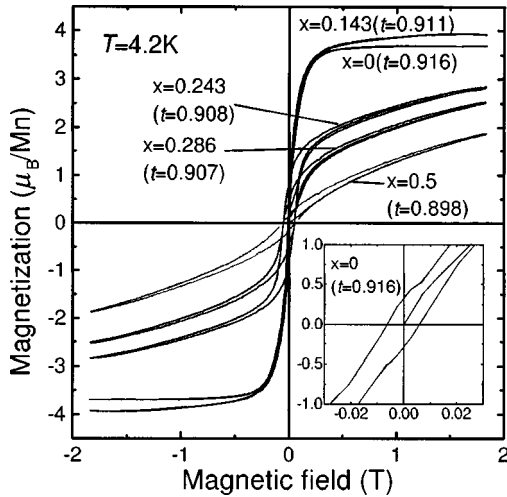
FIG. 4. Magnetization curves of $(La_{1-x}Dy_x)_{0.7}Ca_{0.3}MnO_3$ ($0 \leqslant x \leqslant 0.5$) obtained for magnetic fields of up to 1.8 T at 4.2 K. The inset shows the enlargement of magnetization curve of $(La_{1-x}Dy_x)_{0.7}Ca_{0.3}MnO_3$ ($x=0$).

FIG. 5. Magnetization curves of $(La_{1-x}Dy_x)_{0.7}Ca_{0.3}MnO_3$ ($x=0.143$) obtained for magnetic fields of up to 53 T at 77 and 4.2 K.

termined as a temperature where the second cusp appears (indicated with a double arrow in the present study). In this way, we found that the present compounds for $x=0.143$, 0.243, and 0.286 ($t=0.911$, 0.908, and 0.907) become the reentrant spin glass. It should be noted that T_g's for the compounds of $x=0.143$, 0.243, and 0.286 ($t=0.911$, 0.908, and 0.907) correspond to the temperatures where the resistivity increases again (indicated with a double arrow in Fig. 2). This suggests that the cause of the increase in electrical resistivity below T_g is collapse of the ferromagnetic ordering to reduce the mean free path of e_g electrons. The relation between T_C and tolerance factor will be discussed later.

For all the compounds, magnetization measurements have been made by applying magnetic fields up to 1.8 T. Typical results at 4.2 K are shown in Fig. 4. It is noted that the magnetization for the compound of $x=0$ ($t=0.916$) is saturated at 1.8 T with the value of $3.7\mu_B$. This value is in good agreement with theoretically calculated value of $3.7\mu_B$. Incidentally, the enlargement of magnetization curve of $x=0$ ($t=0.916$) around zero field is shown in the inset of this figure. As seen in the inset, there is a hysteresis in the magnetization curve. This suggests that irreversible domain-wall displacement occurs even with a magnetic field below 0.01 T.

The magnetization of the compound of $x=0.143$ ($t=0.911$) is not saturated and is larger than that of the compounds of $x=0$ ($t=0.916$). In order to measure the saturated moment in the compound of $x=0.143$ ($t=0.911$), we applied pulsed high magnetic fields up to 53 T (pulse duration of 8 ms) to the compound at 4.2 and 77 K. The obtained magnetization curves are shown in Fig. 5. As known from the figure, the magnetization is not saturated even at 53 T for both the temperatures. The magnetization for 53 T at 4.2 K is obtained to be $4.4\mu_B$, but this value is larger than the value of $3.7\mu_B$ [the measured value for $x=0$ ($t=0.916$), mentioned above]. This difference is probably due to the existence of the magnetic moment of Dy^{3+} besides that of Mn^{3+} and Mn^{4+}. In fact, the value of magnetization including the moment of Dy^{3+} ($4.7\mu_B$) is almost the same as the experi-

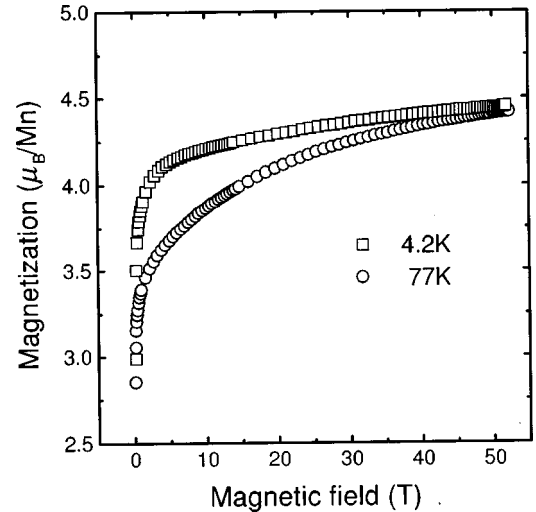mental one. The magnetization curves for the compounds of $x=0.243$, 0.286, and 0.5 ($t=0.908$, 0.907, and 0.898) are quite different from that of the compound for $x=0$ ($t=0.916$); that is, they show a large hysteresis and their magnetizations at 1.8 T are quite low. These features may be mainly related to the fact that the compound of $x=0.243$, 0.286, and 0.5 ($t=0.908$, 0.907, and 0.898) exhibits a spin glass state, as mentioned before.

We have measured the magnetoresistance (MR) by applying magnetic fields up to 8 T at 77 and 4.2 K for all the compounds. MR normalized by zero-field value ρ/ρ_0 is shown in Figs. 6(a) (77 K) and 6(b) (4.2 K). As known from Fig. 6(a), colossal magnetoresistance (CMR) is observed for all the compounds. At 77 K, the maximum decrease of ρ/ρ_0 ($\sim 10^3$) is observed for $x=0.243$ ($t=0.908$). This is because T_C of the compound is closest to 77 K among the present compounds and therefore MR change by an applied magnetic field is most significant.[2,3] Similarly, in Fig. 6(b), CMR is observed for all the compounds, but the curves of $x=0.243$ and 0.286 ($t=0.908$ and 0.907) have a large hysteresis. This is because these compounds become spin glass at 4.2 K, as mentioned in Fig. 3.

A characteristic feature noted in Figs. 6(a) and 6(b) is that MR decreases rapidly for the initial increment of magnetic field of less than 0.2 T for all the compounds. In order to see the rapid decrease in more detail, typical results for $x=0$, 0.071, and 0.143 ($t=0.916$, 0.914, and 0.911) are enlarged and shown in Figs. 7(a), 7(b), and 7(c), respectively, where the solid and dotted lines represent MR at 77 K and 4.2 K, respectively. As is found in the figures, the decrease in ρ/ρ_0 is about 20–30 % at 0.2 T for every compound. The order of decrease is comparable to that of GMR observed in multilayer and granular thin films.[17] Moreover, such decrease at 4.2 K is larger than that at 77 K seen in Figs. 7(a) and 7(b). Hwang *et al.*[18] have found similar rapid decrease for $La_{1/3}Sr_{2/3}MnO_3$ and they interpreted this rapid decrease as tunneling magnetoresistance (TMR);[19] that is, spin-polarized tunneling between grains exists and dominates MR when CMR is relatively small. We believe that the rapid decrease observed in the present compounds is also due to TMR.
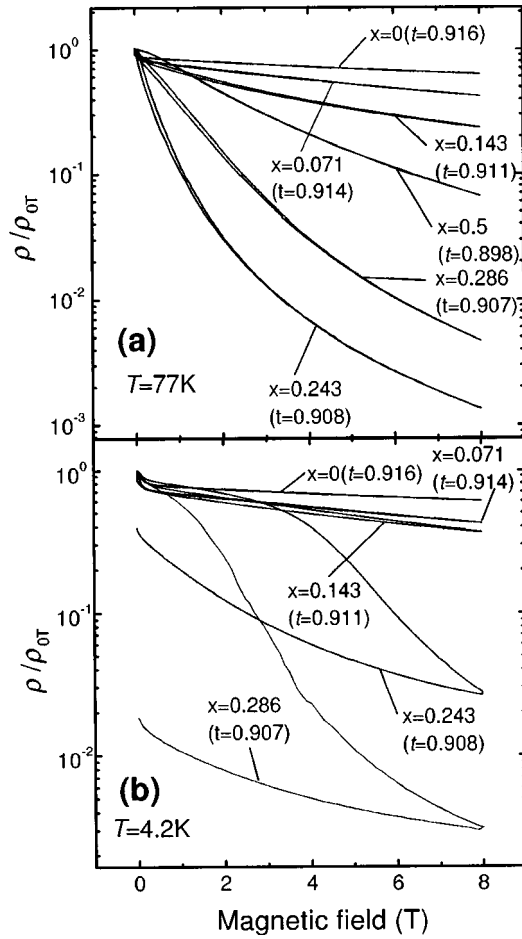
FIG. 6. Magnetoresistance curves of $(La_{1-x}Dy_x)_{0.7}Ca_{0.3}MnO_3$ $(0 \leq x \leq 0.5)$ obtained for magnetic fields of up to 8 T at 77 K (a) and 4.2 K (b).

FIG. 7. Magnetoresistance against magnetic fields of $(La_{1-x}Dy_x)_{0.7}Ca_{0.3}MnO_3$ up to 8 T. (a) $x=0$. (b) $x=0.071$. (c) $x=0.143$. Solid and dotted lines represent magnetoresistances at 77 and 4.2 K, respectively.

IV. DISCUSSION

Figure 8 shows T_C and T_g of $(La_{1-x}Dy_x)_{0.7}Ca_{0.3}MnO_3$ as a function of tolerance factor t calculated using ionic radii reported by Shannon.[20] The figure also shows T_C and T_g of $(La-Tb)_{2/3}Ca_{1/3}MnO_3$ obtained by Teresa et al.,[9] and T_C of $(La-Pr)_{0.7}Ca_{0.3}MnO_3$ and $(La-Y)_{0.7}Ca_{0.3}MnO_3$ obtained by Hwang et al.[3]

In the figure, the electronic and magnetic states in the present compounds are also shown by using notations derived by Hwang et al.[3] and Teresa et al.;[9] that is, paramagnetic insulator (PMI), ferromagnetic metal (FMM), and spin glass insulator (SGI).

As known from the figure, when t is larger than 0.913, the relation between T_C and t of $(La-Dy)_{0.7}Ca_{0.3}MnO_3$ is almost the same as those of $(La-Tb)_{2/3}Ca_{1/3}MnO_3$, $(La-Pr)_{0.7}Ca_{0.3}MnO_3$ and $(La-Y)_{0.7}Ca_{0.3}MnO_3$. This means that the phase diagram (T_C-t relation) derived by Hwang et al. holds even for the present compound containing heavy rare-earth metal ions, i.e., Dy^{3+} when t is larger than 0.913. When t is smaller than 0.907, a spin glass insulator appears at low temperatures. This spin glass insulator is different from a ferromagnetic insulator that appears in the compounds containing light rare-earth metal ions of Pr^{3+} and/or Y^{3+}. A similar spin glass insulator has also been reported for the compound $(La-Tb)_{2/3}Ca_{1/3}MnO_3$. As was mentioned
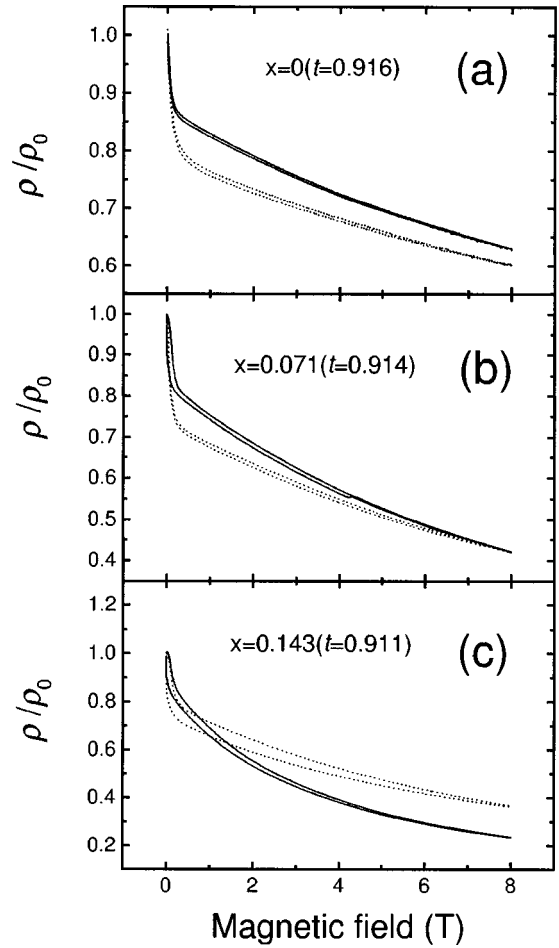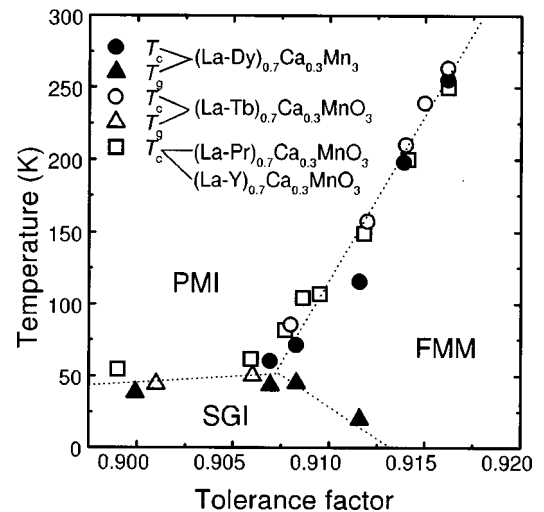

FIG. 8. Electronic and magnetic phase diagram: T_C and T_g as a function of t. Solid circle and solid triangle denote T_C and T_g of $(La-Dy)_{0.7}Ca_{0.3}MnO_3$. Open square denotes T_C of $(La-Pr)_{0.7}Ca_{0.3}MnO_3$, $(La-Y)_{0.7}Ca_{0.3}MnO_3$ obtained by Hwang et al. Open circle and open triangle denote T_C and T_g of $(La-Tb)_{2/3}Ca_{1/3}MnO_3$ obtained by Teresa et al.

before, we found that the reentrant spin glass state appears for t values between 0.907 and 0.913.

The above difference in magnetic state at low temperatures between $(La_{1-x}Dy_x)_{0.7}Ca_{0.3}MnO_3$ and $(La_{1-x}Pr_x)_{0.7}Ca_{0.3}MnO_3$ indicates that the magnetic state depends not only on the tolerance factor t but also on the difference in size among A-site ions as suggested by Rodriguez-Martinez and Attfield.[14] Rodriguez-Martinez and Attfield[14] and Damay *et al.*[15] have used the variance (second moment) of the A-site ions radii distribution σ^2 to quantify the effect of the difference in size among A-site ions. They have defined σ^2 as $\sigma^2 = \Sigma y_i r_i^2 - \langle r_i \rangle^2$, where i is the difference of the three kinds of A-site ions, r_i is the radius of each A-site ion, y_i is their fractional occupancies of the i ions ($\Sigma y_i = 1$), and $\langle r_i \rangle$ is the average radius of A-site ions. When we have calculated σ^2 for $(La_{1-x}Dy_x)_{0.7}Ca_{0.3}MnO_3$ and $(La_{1-x}Pr_x)_{0.7}Ca_{0.3}MnO_3$, we found that the σ^2 of $(La_{1-x}Pr_x)_{0.7}Ca_{0.3}MnO_3$ is almost constant and small ($\sim 5.0 \times 10^{-6}$ nm^2). However, the σ^2 of $(La_{1-x}Dy_x)_{0.7}Ca_{0.3}MnO_3$ increases with increasing Dy^{3+} content; that is from 5.0×10^{-6} nm^2 for $x=0$ to 3.0×10^{-5} nm^2 for $x=0.5$. This difference in value of σ^2 between $(La_{1-x}Dy_x)_{0.7}Ca_{0.3}MnO_3$ and $(La_{1-x}Pr_x)_{0.7}Ca_{0.3}MnO_3$ clearly indicates that the difference in size among A-site ions plays an important role in determining magnetic state. The calculation also shows that the spin glass state appears when σ^2 is larger than about 1.5×10^{-5} nm^2. We speculate from the above result that a large value of σ^2 ($1.5 \sim 3.0 \times 10^{-5}$ nm^2) corresponds to a random distribution of the Mn-O-Mn bond angle and this randomness suppresses the transfer energy between Mn atoms leading the spin glass state. A more detailed mechanism of the spin glass state has to be made clear in the future.

Next, we discuss the electrical resistivity above T_C for the present compounds. In that temperature range, electrical resistivity for manganite compounds is known to be proportional to $1/T^{1/4}$. This is explained by the variable-range hopping mechanism suggested by Mott.[21] In fact, Khazeni *et*
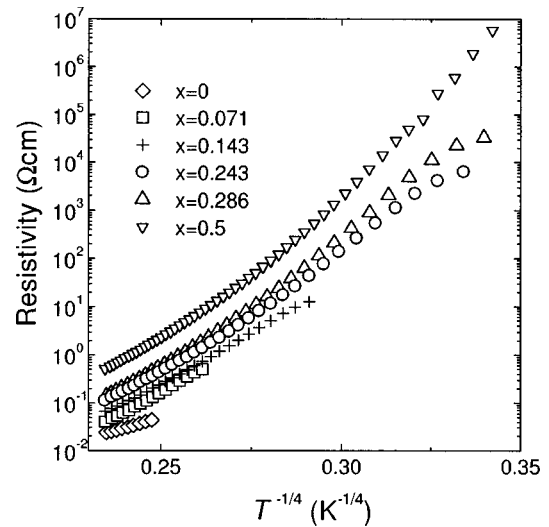

FIG. 9. $\log \rho$ vs $1/T^{1/4}$ plot for the specimens of $(La_{1-x}Dy_x)_{0.7}Ca_{0.3}MnO_3$ ($0 \leq x \leq 0.5$).

al.[22] confirmed its validity for $Nd_{0.62}Pb_{0.3}MnO_3$ single crystal. Therefore, we plotted $\log \rho$ against $1/T^{1/4}$ for temperatures above T_C for all the compounds as shown in Fig. 9. It should be noted in the figure that the $\log \rho$ is nearly proportional to $1/T^{1/4}$ for all compounds when $1/T^{1/4}$ is smaller than about 0.28, but it deviates from the linear relation when $1/T^{1/4}$ exceeds 0.28. This indicates that the present temperature dependence results not only from variable-range hopping of electrons but, in addition, from another origin that is related to grain boundaries. The details of the mechanism should be made clear in the future.

ACKNOWLEDGMENT

[1] G. H. Jonker and J. H. van Santen, Physica (Amsterdam) **16**, 337 (1950).

[2] A. Urushibara, Y. Moritomo, T. Arima, A. Asamitsu, G. Kido, and Y. Tokura, Phys. Rev. B **51**, 14 103 (1995).

[3] H. Y. Hwang, S-W. Choeng, P. G. Radaelli, M. Marezio, and B. Batlogg, Phys. Rev. Lett. **75**, 914 (1995).

[4] P. G. Radaelli, D. E. Cox, M. Marezio, S-W. Choeng, P. E. Schiffer, and A. P. Ramirez, Phys. Rev. Lett. **75**, 4488 (1995).

[5] J. Barratt, M. R. Lees, G. Balakrishnan, and D. McK Paul, Appl. Phys. Lett. **68**, 424 (1996).

[6] A. Maignan, Ch. Simon, V. Caignaert, and B. Raveau, J. Magn. Magn. Mater. **152**, 5 (1996).

[7] H. Yoshizawa, R. Kajimato, H. Kawano, Y. Tomioka, and Y. Tokura, Phys. Rev. B **55**, 2729 (1997).

[8] J. Fontcuberta, B. Martínez, A. Seffar, S. Piñol, J. L. García-Muñoz, and X. Obradors, Phys. Rev. Lett. **76**, 1122 (1996).

[9] J. M. De Teresa, M. R. Ibarra, J. Blasco, C. Ritter, P. A. Algarabel, C. Marquina, and A. del Moral, Phys. Rev. Lett. **76**, 3392 (1996).

[10] J. Blasco, J. Garca, J. M. De Teresa, M. R. Ibarra, P. A. Algarabel, and C. Marquina, J. Phys.: Condens. Matter **8**, 7427 (1996).

[11] C. Zener, Phys. Rev. **82**, 403 (1951).

[12] P.-G. de Gennes, Phys. Rev. **118**, 141 (1960).

[13] P. W. Anderson and H. Hasegawa, Phys. Rev. **100**, 675 (1955).

[14] L. M. Rodriguez-Martinez and J. P. Attfield, Phys. Rev. B **54**, 15 622 (1996).

[15] F. Damay, C. Martin, A. Maignan, and B. Raveau, J. Appl. Phys. **82**, 6181 (1997).

[16] B. R. Coles, B. V. B. Sarkissian, and R. H. Taylor, Philos. Mag. B **37**, 489 (1978).

[17] S. Mitani, K. Takanashi, and H. Fujimori, Solid State Phys. **32**, 231 (1997).

[18] H. Y. Hwang, S-W. Cheong, N. P. Ong, and B. Batlogg, Phys. Rev. Lett. **77**, 2041 (1996).

[19] J. S. Helman and B. Abeles, Phys. Rev. Lett. **37**, 1429 (1976).

[20] R. D. Shannon, Acta Crystallogr., Sect. A: Cryst. Phys., Diffr., Theor. Gen. Crystallogr. **32**, 751 (1976).

[21] N. F. Mott, J. Non-Cryst. Solids **1**, 1 (1968).

[22] K. Khazeni, Y. X. Jia, Vincent H. Crespi, L. Lu, A. Zettl, and Marvin L. Cohen, J. Phys.: Condens. Matter **8**, 7723 (1996).